Conductance of a finite missing hydrogen atomic line on Si(001)-(2×1)-*H*

P. Doumergue
CEMES, CNRS, 29 rue J. Marvig, F-31055 Toulouse Cedex, France

L. Pizzagalli
Institute of Physics, Basel University, Klingelbergstrasse 82, CH-4056 Basel, Switzerland

C. Joachim and A. Altibelli
CEMES, CNRS, 29 rue J. Marvig, F-31055 Toulouse Cedex, France

A. Baratoff
Institute of Physics, Basel University, Klingelbergstrasse 82, CH-4056 Basel, Switzerland
(Received 11 February 1999)

We present the results of a calculation of zero-temperature elastic conductance through a finite ''atomic wire'' between Au pads, all supported by a Si(001)-(2×1)-*H* surface. The atomic wire consists of a line of dangling bonds which can be fabricated by removing hydrogen atoms by applying voltage pulses to a scanning tunneling microscopy (STM) tip along one side of a row of H-passivated silicon dimers. Two different line configurations, without and with Peierls distortion, have been considered. We find that the nondistorted line behaves like a single ballistic transmission channel. Conversely, with Peierls distortion present, tunneling occurs through the small resulting energy gap (0.2 eV), leading to inverse decay length of the current of 0.09 Å^{-1}. The conductance of the substrate between the pads without the defect line has also been calculated. In this case, tunneling occurs through a much wider energy gap and a larger inverse decay length of 0.41 Å^{-1}. These fully three-dimensional atomistic computations represent an application of the electron-scattering quantum-chemistry method which was previously used to calculate the conductance of ''molecular wires'' and of STM junctions with various adsorbates. Compared to molecular wires previously investigated by the same method, the atomic wire studied here exhibits the smallest inverse decay length. [S0163-1829(99)09123-7]

I. INTRODUCTION

There is an increasing interest in fabricating atomic-scale nanostructures for fundamental research[1] and for applications like further miniaturization of electronic devices.[2] Several studies have revealed the ability of the scanning tunneling microscope (STM) to modify surface structure in controlled ways on an atomic scale. Thus adsorbed atoms can be moved one by one,[3,4] or removed selectively to create artificial patterns,[5,6] in particular atomic lines.[7,8] Up to now, however, even the properties of such an isolated atomic wire have not been completely known. The eventual use and the experimental characterization of such nanowires is difficult because they must be contacted to perform electrical measurements.[9] From a theoretical point of view, the electronic properties of finite atomic wires (one atom in section) between two electrodes have usually been calculated for free-standing wires, consisting of one,[10,11] two,[12,13] or several atoms.[14–18] In this case, they are assumed frozen in a linear extended form, although the cohesion of the material may in fact favor a more compact configuration of the available atoms. Though short free-standing wires can actually be made between a STM tip and the surface of a suitable sample,[19] useful atomic wires must ultimately be stabilized by bonding to a solid substrate. The underlying material imposes a particular conformation and orbital configuration along the atomic wire which may be different from the idealized one, so that the surface leakage paths must be estimated. Band structure calculations of infinite supported wires have been performed.[20,21] In this case, the effect of the underlying surface is fully considered. However, to progress further in the analysis, while staying close to reality, theoretical studies must take into account both the substrate and the contacting pads which add some contact resistance to any finite-size device.

Several groups have reported the observation of atomic-scale lines. Thus Nogami reported the formation of single-atom wide atomic lines of Ga, In, Sn, and Al on the Si(001) surface at low coverage and even at room temperature (RT).[22] Pb atomic lines can also be grown on this surface.[23] Different systems and supporting substrates are possible: thus Cu wires have been observed on the Pd(110) surface,[24] and isolated lines of Si-dimers appear on β SiC(001) upon partial evaporation of silicon, starting from the Si-rich 3×2 reconstruction.[25]

A particularly interesting kind of atomic-scale line can be made on the monohydride Si(001)-(2×1)-*H* surface using a STM in ultrahigh vacuum by applying voltage pulses across the STM junction to selectively desorb hydrogen atoms along a dimer row.[7] This creates a *dangling-bond* (DB) wire because each dehydrogenated silicon atom carries one dangling orbital. Such DB wires have been experimentally found to be metallic at room temperature,[26–28] each DB creating a surface state in the energy gap. At low temperature, a Peierls distortion[29] occurs, stabilizing a semiconducting structure by opening a small gap at the Fermi level. Up to now, nondis-

torted supported infinite wires have been investigated by band-structure calculations,[21] but not the electrical properties of finite atomic wires, whether Peierls distorted or nondistorted. Moreover, the resulting reactive DB structure can presumably be used as a trap for other species, and thus to form different kinds of atomic wires.[21,8,30]

In this paper, the length dependence of the conductance of a DB line stabilized on a Si(001)-(2×1)-*H* surface is investigated in detail. The influence of the contacting pads and the finite line length are fully taken into account together with the complete atomistic and electronic structure of the line and of the supporting substrate. Electron-electron and electron-phonon interactions, inelastic scattering, and finite-temperature effects are not included. The conductance of planar Au pad–[Si(100)-(2×1)-*H*]–Au pad junctions is calculated with and without the atomic DB line. The conductance of the full hydrogen-passivated substrate decreases exponentially with the distance between the two pads, as expected for an insulating surface. In the presence of the DB line, the one-dimensional electronic band structure of the latter is progressively recovered with increasing length. If Peierls distortion is taken into account, the *I*-*V* characteristic of the chain is linear at low voltage, but its conductance is determined by tunneling, and decreases exponentially, albeit with a relatively small inverse decay length γ of 0.09 Å^{-1}.

II. MODELS

Our conductance calculations were performed with the elastic-scattering quantum-chemistry (ESQC) method.[31] The advantage of this technique is its ability to calculate exactly the scattering by a complex inhomogeneous subsystem or defect embedded in a periodic system. Here we deal with a finite supported atomic wire contacted by metallic pads, taking into account the valence electronic structure of the wire, of the substrate, and of the pads in a lowest combination of atomic orbitals representation. In this way, effects due to the finite size of the wire, to the contact resistance between the wire and the pads, and to the coupling with the substrate are considered. Figure 1 shows the ''defect'' which contains the metal-atomic wire-metal junction of interest and part of the substrate. It includes the edges of the gold pads and a seven layers silicon slab with an ideal 1×1 hydrogen-passivated bottom surface (dihydride) approximately simulating bulk silicon, and a passivated 2×1 top surface (monohydride). The top silicon layers accommodates four dimers in the transverse direction in the defect part, in order to make lateral wire-wire image interactions essentially negligible when applying periodic boundary conditions. Several interpad distances have been considered, encompassing 1–11 dimers along the wire direction. The periodic system on both sides of this defect is composed of the gold pad layers, the seven-layer silicon slab, and the dihydride layer at the bottom. Bloch states propagating in the plane of this system define the incoming and scattered states with respect to which transmission amplitudes and the conductance are calculated. For a long wire, the scattering states of such a complex system cannot at present be calculated on an *ab initio* level. For example, the number of atoms required to calculate the conductance of the 11 missing hydrogen atomic line is about 1100 atoms (defect part) for 5-nm-wide contacting pads.

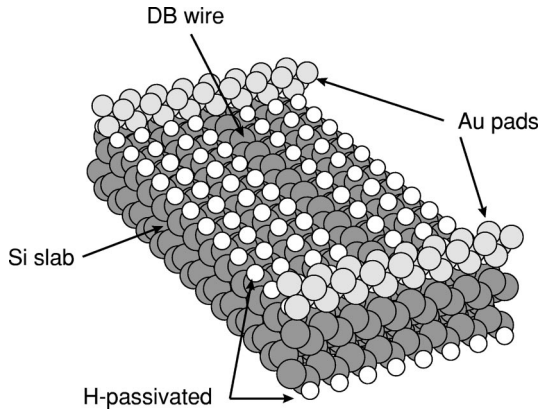

FIG. 1. Model of the metal-atomic wire-metal junction (defect) used in the ESQC calculation of the conductance of a wire consisting of 11 dangling bonds on depassivated silicon surface atoms. The dark gray spheres represent silicon atoms, while the light gray ones show the gold atoms of the contact pads. Both sides of the slab are saturated with hydrogen (white spheres), except along the defect line.

Therefore, a semiempirical approximation, the extended Hückel molecular orbitals (EHMO) model,[32] has been used to construct the full electronic Hamiltonian of the junction. With suitable parametrization, this formalism, originally derived to calculate properties of molecules, has also been found to reasonably reproduce the characteristic features in the electronic structure of silicon surfaces.[33]

In addition to conductance calculations with ESQC, we also performed band-structure calculations using the EHMACC program from the package of Whangbo *et al.*[34] The Si(100)-(2×1)-*H* surface with the DB atomic line was then represented by a similar slab of seven layers, containing four Si atoms perpendicular to the DB line but only two Si atoms along it with periodic boundary conditions applied in plane. This 4×2 supercell is nevertheless large enough (i) to significantly suppress the defect-defect interaction mentioned, and (ii) to allow a Peierls distortion along the defect atomic line.

The EHMO parameters were the same both in the band structure and in the ESQC calculations. This parametrization has been optimized as followed. Starting from standard EHMO semiempirical parameters for Si, the well-known band structure of Si bulk was first recovered using the Nishida parametrization,[35,36] i.e., modifying the Wolfsberg-Helmholz parameters for each type of interaction. A subsequent reparametrization of Si atoms was done so as to reproduce the surface electronic structure local-density-approximation (LDA) calculation[37] of the Si(100)-(2×1) symmetric and $c(4\times2)$ buckled dimer reconstructions. Compared to the bulk parametrization, only the Si $3p$ exponent was slightly modified to take into account the diffuseness of the Si($3p$) surface-atom orbitals. With this parametrization, the Si(100)-(2×1) surface is found to be metallic, whereas a gap of 0.6 eV opens when the buckled $c(4\times2)$ structure is imposed, as expected.[37,38] With the same parameters, the Si(100)-(2×1)-*H* monohydride surface is found to be insulating with a gap of about 2 eV. Finally, the band structure of the one-dimensional surface states derived from the dangling bonds along the missing hydrogen atomic line, as calculated by Watanabe *et al.*,[21] was reproduced via a rep-

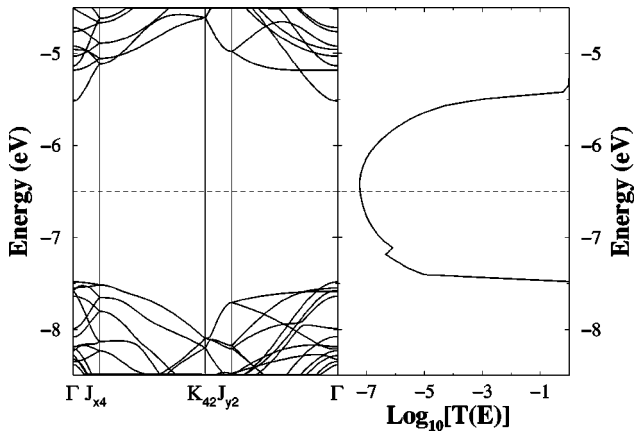

FIG. 2. Left panel: Calculated energy band structure of the slab representing the Si(001)-(2×1)-*H* substrate along the symmetry axis of the Brillouin zone corresponding to our 4×2 computational cell, following the notation of Watanabe *et al.* (Ref. 21). Right panel: Calculated decimal logarithm of the transmission coefficient between two Au film pads separated by 27 Å (six Si dimers) as a function of energy. The dashed line shows the position of the Fermi energy.

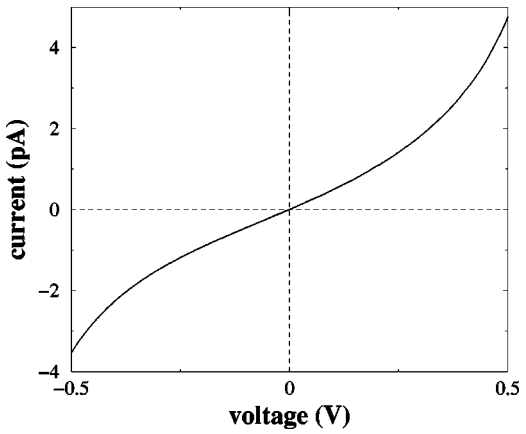

FIG. 3. Calculated current-voltage (*I*-*V*) characteristic of the Si(001)-(2×1)-*H* substrate between Au film pads separated by 27 Å (six dimers).

arametrization of the depassivated Si atoms on one side of the dimer row. This systematic reparametrization procedure was required to achieve a good description of the electronic structure of the supported atomic line, a prerequisite for a viable conductance calculation.

III. PERFECT HYDROGENATED SUBSTRATE

We first consider the band structure and conductance of junctions with the perfect, fully hydrogenated substrate, i.e., without the DB wire, between the two pads. Although all dangling bonds are passivated, the Si(100)-(2×1)-*H* surface is terminated by symmetric dimers, each surface silicon atom being bonded to a neighbor and to a single hydrogen atom.[39] These dimers can be distinguished from those on the clean Si(001) surface by their appearance in STM images and spectra.[40–42] The calculated band structure for the corresponding slab is shown on the left panel of Fig. 2. It exhibits a gap of about 2 eV, in agreement with a previous calculation,[43] if we consider that with a tight-binding model like ours, the empty surface states are not correctly located and are shifted above the bottom of the conduction band. The electronic band structure of the substrate is reflected in the energy dependence of the transmissivity of a finite length junction (right panel, Fig. 2) which can in turn be related to its tunneling spectrum. A transmission coefficient equal to unity is obtained in the range where energy bands and propagating Bloch states exist, i.e., within the valence and conduction bands in our case. However, within the electronic band gap, the transmissivity is significantly reduced (note the log scale).

Since the substrate exhibits a relatively wide gap, the junction current-voltage characteristic (*I*-*V*) is linear over a large range of bias voltage (Fig. 3). In this linear regime, transport occurs by nonresonant tunneling mainly via the tails of the surface states, broadened by their interactions with the contacting pads. As a consequence of the underlying tunneling phenomenon, the conductance of the junction decreases exponentially when the electrode separation is increased, as can be seen in Fig. 4. The variation of the total transmission coefficient at the Fermi energy is well described by the expression

$$T(d) = T_0 e^{-\gamma d}, \tag{1}$$

expected to be valid for tunneling in the limit $\gamma d \ll 1$, and recently used to fit transmission through different ''molecular wires.''[44] Here γ and d, respectively, are the inverse decay length and the interpad distance; we find $\gamma = 0.41$ Å^{-1}, which is smaller than for tunneling through vacuum ($\gamma = 2.21$ Å^{-1}). Using the expression

$$\frac{I}{V} = \frac{e^2}{\pi\hbar} T(d), \tag{2}$$

which describes the conductance measured between voltage probes far from the contacts, i.e., in equilibrium,[45] we find that for an interpad distance of 5 nm and an applied voltage of 1 mV, the current in the junction is lower than 10^{-4} pA.

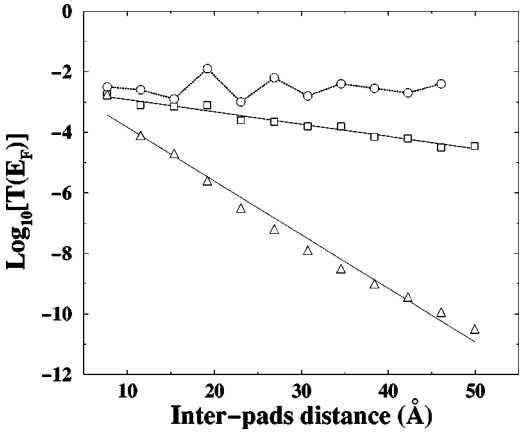

FIG. 4. Variation of the decimal logarithm of the transmission coefficient at the Fermi level as a function of the distance between the two pads, in the case of the perfect Si(001)-(2×1)-*H* substrate (triangles), of the undistorted DB wire (circles), and of the Peierls-distorted DB wire (squares). The solid lines are linear fits. Note that there is no significant decrease for the metallic undistorted DB wire, although the net transmissivity is much smaller than one.

TABLE I. EHMO calculated electronic band gap E_g and inverse decay length γ of the tunneling current for several atomic and molecular wires.

Wire type	Ref.	E_g (eV)	γ (Å^{-1})
$(Xe)_n$	13	9	0.74
alkane chain	51	8.9	0.85
Si(001)-(2×1)-*H*	this work	2	0.41
oligothiophenes	51	1.53	0.33
polyenes	51	1.11	0.19
DB wires	this work	0.2	0.09

It is instructive to compare γ to the values obtained for molecular wires. On the Si(001)-(2×1)-*H* surface each fully hydrogenated dimer row can be approximately viewed as formed by two chains of sp^3-bonded Si atoms. Consequently, each row may be compared to an alkane chain $(CH_2)_n$. On the one hand, the overall 2-eV band gap of the system under consideration is much smaller than that of an alkane chain (8.9 eV), thus favoring a slower decay (see Table I). On the other hand, the Si atoms are further apart along the dimer row (3.84 Å) compared to equivalent carbon atoms along the alkane chain (2.51 Å), so that the reduction in conductance per structural unit is not so strong.

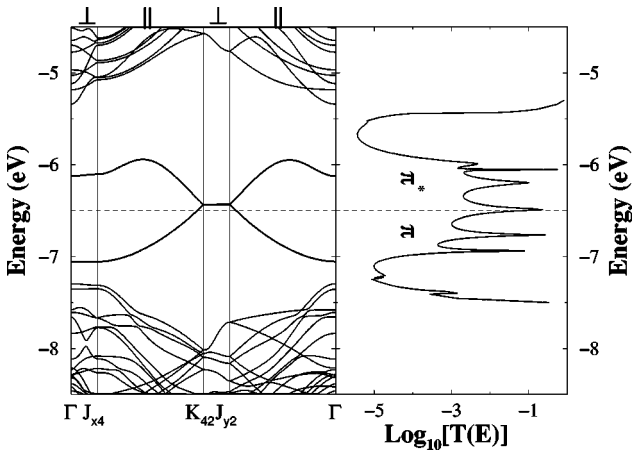

FIG. 5. Left panel: Calculated energy band structure of the Si(001)-(2×1)-*H* slab with an undistorted DB line along the symmetry lines defined in Fig 2. Symbols ⊥ and ∥ indicate directions perpendicular and parallel to the DB line, respectively. Right panel: Calculated decimal logarithm of the transmission coefficient as a function of energy for the DB wire between two Au film pads separated by 27 Å (six dimers), assuming a two-dimers-wide computational cell. The dashed line shows the position of the Fermi energy.

IV. HYDROGENATED SUBSTRATE WITH A DEPASSIVATED LINE

We now consider results obtained in the presence of a DB line on the Si(100)-(2×1)-*H* substrate. One row of hydrogens is replaced by a row of Si dangling-bond orbitals. Recent scanning tunneling spectroscopy measurements at room temperature by Hitosugi *et al.*[28] on rather long DB wires show a finite density of states at the Fermi level (zero voltage) if it is sufficiently perfect; this is compatible with metallic conduction along such a defect line. Previous LDA band-structure calculations for perfect infinite DB wires predicted the metallic behavior,[21] the creation of the DB line being associated with emergence of a quasi-one-dimensional band crossing the Fermi level. In our conductance calculations for the finite line, we have used the relaxed structure of the infinite line calculated by Watanabe *et al.*,[21] i.e., we have neglected a possible influence of the Au pads on the structure of the wire. Our band-structure calculations confirm the creation of DB-derived bands in the middle of the gap of the Si(100)-(2×1)-*H* band structure (Fig. 5, left). Note that the Brillouin zone corresponding to the 4×1 supercell used by Watanabe *et al.* is twice as long in the direction parallel to the line, so that only a single DB-derived band appears in their Fig. 2(a). In our 4×2 supercell, this band is folded into π and π^*-like bands which become degenerate along the $K_{42}-J_{y2}$ edge. The dispersion of these two bands in the direction perpendicular to the DB line (Γ-J_{x4} and K_{42}-J_{y2} edges) is very small, confirming the essentially one-dimensional (1D) character of the DB-derived electronic states localized around the defect line.

The energy dependence of the transmissivity calculated for a line of six DB's is shown on the right of Fig. 5. To reduce computation time, this spectrum was calculated for a junction only two dimers wide. This reduction produced insignificant changes in test computations done at a few points with the wider junction shown in Fig. 1. Each dangling bond creates a resonance in the tunneling spectrum of the junction. When the length of the wire is increased by incorporating an additional DB, a new resonance appears inside the substrate band gap and the previous ones are slightly redistributed in energy. Differences among the strengths and widths of resonances are due to different coupling either with the pads or with the neighboring substrate atoms. A very narrow (broad) resonance corresponds to an almost decoupled (strongly coupled) orbital. Furthermore, the conductance of the undistorted DB line does not decrease when its length is increased, but merely oscillates reflecting the shifting positions of those resonances with respect to the Fermi level, as seen in Fig. 4. The *I-V* characteristic of the 6-DB wire is presented in Fig. 6. The steps in current arise because sharp resonances successively enter the energy interval explored by the bias voltage. Beyond a certain length of the line, the separation between adjacent resonances will be lower than the thermal energy *kT*. If *kT* is still smaller than the bandwidth, there will then be enough states in the chain to reproduce the dispersion of the DB-derived bands. In this limit, the *I-V* characteristic will become essentially linear. The junction conductance will then be limited only by the pad-wire constriction, since a full ballistic channel will be opened through the line. As long as the line length is lower than the electronic mean free path in the line, the conductance will not noticeably decrease with increasing wire length, and will remain given by Eq. (2) with the transmissivity *T* computed ignoring scattering by possible imperfections in the line, as in our ESQC-based calculations.

Recent STM experiments have revealed the appearance of a new DB wire conformation at low temperature.[27] One of two maxima associated with DB orbitals is alternatively seen in images of empty and occupied states. The authors pro-

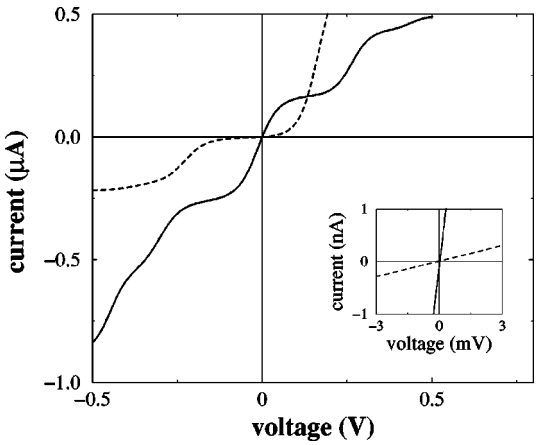

FIG. 6. Calculated I-V characteristics of the supported DB line, connecting two Au film pads 27 Å apart (six dimers). The solid (dashed) curve shows the I-V characteristic of the nondistorted (Peierls-distorted) DB line. The inset is a zoom around the origin.

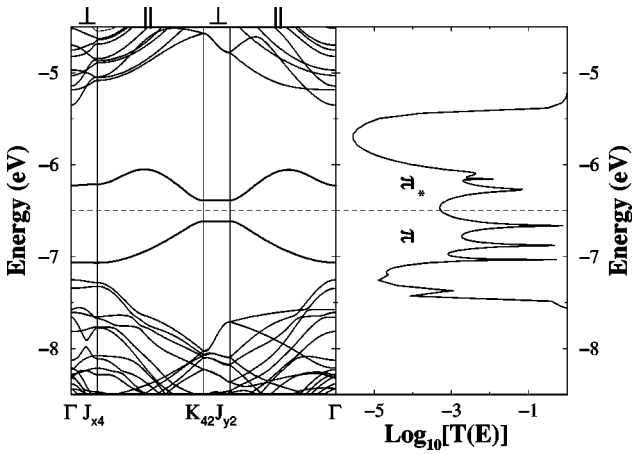

FIG. 7. Left panel: Calculated energy band structure of the Si(001)-(2×1)-H slab with a Peierls-distorted DB line along the symmetry lines, defined in Figs. 2 and 5. Symbols ⊥ and ∥ indicate space directions perpendicular and parallel to the the DB line, respectively. Right panel: Calculated decimal logarithm of the transmission coefficient as a function of energy for a distorted DB wire between two Au film pads separated by 27 Å (six dimers), assuming a two-dimer-wide computational cell. The dashed line shows the position of the Fermi energy.

posed a model where dehydrogenated Si atoms along the line are alternatively raised and lowered in a Peierls-like distortion.[29] This is the result of a competition between a lowering of electronic energy by atomic displacements which lift the degeneracy between the filled π and empty π^* states, and the mechanical distortion of the chain. Many theorists have considered 1D models including electron-phonon and electron-electron interactions leading to dimerizations along the chain.[46] But here, the situation is somewhat different. Without distortion, the π and π^* bands are degenerate along K_{42}-J_{y2} because the associated wave functions have nodes on every second atom along the line. Thus two possible states, differing by a shift of one lattice spacing, are energetically equivalent. This degeneracy can be lifted without much cost in mechanical energy by the proposed up-down distortion. Such a distortion decreases the energy of DB's on lowered atoms (more s character) and increases it on raised atoms (more p_z character). A similar situation occurs in the case of π-bonded surface atoms on the Si(111)-(2×1) surface, except that they form zigzag chains[47,48] as well as for a DB wire on the Si(111)-(1×1)-H surface.[47–49] To include these effects, we have assumed a height difference of 0.1 Å between up and down Si atoms along the wire.[50]

Figure 7 shows the calculated band structure for the infinite wire as well as the energy dependence of the transmissivity for a 6-DB wire in a two-dimer-wide junction. The 0.2-eV Peierls gap between the modified π and π^* states straddles the Fermi level, and causes a reduced transmission in that range in the finite wire. As a result, for low-bias voltage, a tunneling transport regime replaces the previous ballistic regime. This can be seen in the resulting I-V characteristic of the junction (Fig. 6). The I-V remains linear at low voltage, but with a significantly reduced slope. Although this indicates a finite density of states near the Fermi level, the lower conductance is characteristic of a tunneling regime where the states accumulate away from the Fermi level but contribute via their tails to the transmissivity. Accordingly, when the wire length is increased, the conductance decreases. The conductance decreases exponentially with an inverse decay length γ in Eq. (1) of only 0.09 Å^{-1} (Fig. 4). A polyene chain $(CH)_n$ is the simplest molecular wire with an electronic structure similar to that of the DB atomic wire considered here, one p_z orbital of each carbon atom participating in the valence or conduction states of the wire. The corresponding inverse decay length obtained by the same method is reported for comparison in Table I.[51] The gap of the DB wire is about six times smaller than the gap of the polyene molecular wire, but its inverse decay length is only half as small. One might expect to achieve an even better small γ for carefully designed molecular wires with an equivalent small gap, however.[44]

It is sometimes assumed that it is only the smallest gap straddling the Fermi level which controls the tunneling current decay, i.e., that there is a simple proportionality relation between the gap and the inverse decay length γ. In the case of tunneling through the band gap of an insulator or semiconductor, a generalization of the WKB approximation leads to

$$\gamma \simeq \frac{\sqrt{2m^*\Delta E}}{\hbar}, \tag{3}$$

where ΔE is the separation in energy between the Fermi level and the nearest band edge, and m^* the corresponding effective mass in the tunneling direction.[52] ΔE is governed by the occupation of interface states at contacts with the electrodes and may be proportional to the gap for nearly perfect interfaces.[53] On the other hand, m^* is proportional to the gap only if the latter is small compared to the width of the relevant band. Thus γ is approximately proportional to the gap only in that limit. Our more reliable approach takes into account the atomic structure of the contact pads and of the wire. What we have here is another example where the

simple law (3) based on the simple WKB approximation does not well describe tunneling through atomic and molecular wires, especially short ones.[51] In general, details in the superposition of several tunnel channels at the Fermi level determine the inverse decay length.[44]

V. CONCLUSION

In conclusion, we have demonstrated that the length dependence of the conductance of an atomic line on an insulating substrate can be calculated by the ESQC method taking into account the 3D electronic structure of the junction including the substrate and the contacting pads. Considering the perfect passivated Si(001)-(2×1)-*H* substrate without the line, we showed that tunneling transport takes place through a 2-eV gap with an inverse decay length of 0.41 $Å^{-1}$. The effects of a missing hydrogen line has been calculated in two different configurations, with or without Peierls distortion. We found that a single-ballistic-channel regime can develop above a certain temperature or length if the Peierls distortion is suppressed. Otherwise, 1D bands arising from the depassivated dangling bonds along the line are split about the Fermi level, so that at low temperatures transport occurs via tunneling through the small resulting Peierls gap (0.2 eV). The tunneling inverse decay length of such a DB wire is smaller than polyene chains but carefully designed molecular wires are expected to give better results. Additional studies are required to clarify this issue and also whether different systems, in particular wires fabricated by deposing other atomic species near the reactive DB line,[8,30] could provide some improvements.

ACKNOWLEDGMENTS

We thank T. C. Shen, T. Hashizume, T. Onogi, and Y. Wada for discussions about the fabrication and characterization of missing hydrogen atomic lines. This work was done with the computational support of the ''Institut du développement et des ressources en informatique scientifique'' (IDRIS). One of us (L.P.) would like to acknowledge partial support from NFP36 ''Nanosciences'' of the Swiss National Fundation for Research, and Dr. A. J. Fisher for an invitation to present this work at the ESF Conference on Computational Physics for Nanotechnology.

[1] M.F. Crommie, C.P. Lutz, and D.M. Eigler, Science **262**, 218 (1993).
[2] C.F. Quate, Nature (London) **352**, 571 (1991).
[3] D.M. Eigler and E.K. Schweizer, Nature (London) **344**, 524 (1990).
[4] L. Bartels, G. Meyer, and K.-H. Rieder, Phys. Rev. Lett. **79**, 697 (1997).
[5] I.-W. Lyo and P. Avouris, Science **253**, 173 (1991).
[6] A. Kobayashi *et al.*, in *Atomic and Nanometer-Scale Modification of Materials: Fundamentals and Applications*, Vol. 239 of *NATO ASI Series E: Applied Sciences*, edited by P. Avouris (Kluwer, Dordrecht, 1993), p. 37.
[7] T.-C. Shen *et al.*, Science **268**, 1590 (1995).
[8] T. Hashizume, S. Heike, M. I. Lutwyche, S. Watanabe, K. Nakajima, T. Nishi, and Y. Wada, Jpn. J. Appl. Phys. **35**, L1085 (1996).
[9] H. Ohnishi, Y. Kondo, and K. Takayanagi, Nature (London) **395**, 780 (1998).
[10] N.D. Lang, Phys. Rev. B **36**, 8173 (1987).
[11] C. Joachim, X. Bouju, and C. Girard, in *Atomic and Nanometer-Scale Modification of Materials: Fundamentals and Applications*, (Ref. 6), p. 247.
[12] N.D. Lang, Phys. Rev. B **52**, 5335 (1995).
[13] L. Pizzagalli, C. Joachim, X. Bouju, and C. Girard, Europhys. Lett. **38**, 97 (1997).
[14] T.N. Todorov and A.P. Sutton, Phys. Rev. Lett. **70**, 2138 (1993).
[15] M. Brandbyge, J. Schiotz, M. R. Sorensen, P. Stolze, K. W. Jacobsen, J. K. Norskov, L. Olesen, E. Laegsgaard, I. Stensgaard, and F. Besenbacher, Phys. Rev. B **52**, 8499 (1995).
[16] R.N. Barnett and U. Landman, Nature (London) **387**, 788 (1997).
[17] J. Mozos, C. C. Wan, and G. Taraschi, Phys. Rev. B **56**, R4351 (1997).
[18] N.D. Lang and P. Avouris, Phys. Rev. Lett. **81**, 3515 (1998).
[19] A. Yazdani, D.M. Eigler, and N.D. Lang, Science **272**, 1921 (1996).
[20] T. Yamada and Y. Yamamoto, Phys. Rev. B **54**, 1902 (1996).
[21] S. Watanabe, Y.A. Ono, T. Hashizume, and Y. Wada, Phys. Rev. B **54**, R17 308 (1996).
[22] J. Nogami, in *Atomic and Molecular Wires*, Vol. 341 of *NATO ASI Series E: Applied Sciences*, edited by C. Joachim and S. Roth (Kluwer, Dordrecht, 1997), p. 11.
[23] Z.-C. Dong, T. Yakabe, D. Fujita, T. Ohgi, D. Rogers, and H. Nejon, Jpn. J. Appl. Phys., Part 1 **37**, 807 (1998).
[24] J. Bucher, in *Atomic and Molecular Wires*, Vol. 341 of *NATO ASI Series E: Applied Sciences* (Ref. 22), p. 1.
[25] P. Soukiassian, F. Semond, A. Mayne, and G. Dujardin, Phys. Rev. Lett. **79**, 2498 (1997).
[26] T. Hitosugi, T. Hashizume, S. Heike, S. Watanabe, Y. Wada, T. Hasegawa, and K. Kitazawa, Jpn. J. Appl. Phys. **36**, L361 (1997).
[27] T. Hitosugi, T. Hashizume, S. Heike, H. Kajiyama, Y. Wada, S. Watanabe, T. Hasegawa, and K. Kitazawa, J. Surf. Anal. **3**, 312 (1998).
[28] T. Hitosugi, T. Hashizume, S. Hieke, Y. Wada, S. Watanabe, T. Hasegawa, and K. Kitazawa, Appl. Phys. A: Mater. Sci. Process. **66**, S695 (1998).
[29] R. E. Peierls, *Quantum Theory of Solids* (Oxford University Press, London, 1955).
[30] A. Yajima, M. Tsukada, S. Watanabe, M. Ichimura, Y. Suwa, T. Onogi, and T. Hashizume (unpublished).
[31] P. Sautet and C. Joachim, Phys. Rev. B **38**, 12 238 (1988).
[32] R. Hoffmann, J. Chem. Phys. **39**, 1397 (1963).
[33] S. Ciraci and H. Wagner, Phys. Rev. B **27**, 5180 (1983).
[34] M.-H. Whangbo *et al.*, *QCPE # 571*, Extended-Hückel Molecular, Crystal and Properties Package, Quantum Chemical Program Exchange, 1989.
[35] M. Nishida, J. Phys. C **11**, 1217 (1978).
[36] M. Nishida, J. Chem. Phys. **69**, 956 (1978).
[37] A. Ramstad, G. Brocks, and P.J. Kelly, Phys. Rev. B **51**, 14 504 (1995).

[38] J.E. Northrup, Phys. Rev. B **47**, 10 032 (1993).
[39] J.J. Boland, Phys. Rev. Lett. **65**, 3325 (1990).
[40] R.J. Hamers, P. Avouris, and F. Bozso, Phys. Rev. Lett. **59**, 2071 (1987).
[41] J.J. Boland, Phys. Rev. Lett. **67**, 1539 (1991).
[42] J.J. Boland, Phys. Rev. B **44**, 1383 (1991).
[43] S. Ciraci, R. Butz, E.M. Oellig, and H. Wagner, Phys. Rev. B **30**, 711 (1984).
[44] M. Magoga and C. Joachim, Phys. Rev. B **57**, 1820 (1998).
[45] R. Landauer, Z. Phys. B **68**, 217 (1987).
[46] For a recent review, see J. Voit, Rep. Prog. Phys. **58**, 977 (1995).
[47] K.C. Pandey, Phys. Rev. Lett. **47**, 1913 (1981).
[48] R.M. Feenstra and M.A. Lutz, Phys. Rev. B **42**, 5391 (1990).
[49] S. Watanabe, Y.A. Ono, T. Hashizume, Y. Wada, J. Yamauchi, and M. Tsukada Phys. Rev. B **52**, 10 768 (1995).
[50] Y. Wada (private communication).
[51] M. Magoga and C. Joachim, Phys. Rev. B **56**, 4722 (1997).
[52] C. B. Duke, *Tunneling in Solids* (Academic, New York, 1962).
[53] J. Tersoff, Phys. Rev. B **30**, 4874 (1984).